η^1-Coordination of Phosphinine to Chromium, Molybdenum, and Tungsten†,[1]

Christoph Elschenbroich,* Steffen Voss, Olav Schiemann, Andrea Lippek, and Klaus Harms

Fachbereich Chemie der Philipps-Universität, D-35042 Marburg, Germany

Received June 15, 1998

The homoleptic complexes hexakis(η^1-phosphinine)molybdenum **10** and hexakis(η^1-phosphinine)tungsten **11** have been prepared via reduction of suitable metal halides with magnesium or zinc in order to explore trends in the triad $(\eta^1\text{-}C_5H_5E)_6M$, M = Cr, Mo, W. According to X-ray crystal structure determinations, **10** and **11** are isostructural and show almost ideal octahedral geometry of the metal−phosphorus core. The bond distances *d*(M−P) are relatively short in comparison to other homoleptic phosphane complexes of Mo and W; they follow the expected order: Cr−P (2.26 Å, **2**) < Mo−P (2.38 Å, **10**) ≈ W−P (2.37 Å, **11**). The NMR data exhibit the same trends upon the η^1-coordination of phosphinine as hexakis(η^1-phosphinine)chromium **2**, but the change of the central metal from Cr to W results in an increased shielding of the neighboring atoms (P, *ortho*-H, and C) of the ligands. The UV−vis spectra of **10** and **11** in comparison to **2** display a continuous hypsochromic shift in the MLCT region. Conversely, the redox potentials for the couples $ML_6^{(+/0)}$, which are increasingly anodic following the sequence Cr < W < Mo, show a discontinuous gradation.

Introduction

The group 15 heteroarenes C_5H_5E (E = N, P, As, Sb, Bi) are ambidentate ligands and as such pose the question of their preferred coordination mode—η^1 (via the lone pair at E) or η^6 (via the π-electrons of the aromatic ring)—depending on the nature of E and the respective central metal. We have shown in the past that for the third-row transition metals phosphinine prefers to bind via the π-orbitals of the aromatic ring (π, η^6) to the early members and via the lone pair (σ, η^1) to the late members. The preparation of $V(\eta^6\text{-}C_5H_5P)_2$ **1**,[2] $Cr(\eta^1\text{-}C_5H_5P)_6$ **2**,[3] $Fe(\eta^1\text{-}C_5H_5P)_5$ **3**,[4] and $Ni(\eta^1\text{-}C_5H_5P)_4$ **4**[5] attests to this notion. However, as for pyridine, the coordination mode of phosphinine derivatives also shows a dependence on the steric demand of the *ortho*-substituents. Hence, cocondensation of 2,6-$(SiMe_3)_2$-pyridine and 2,4,6-$(^tBu)_3$-phosphinine with chromium leads to bis[2,6-$(Me_3Si)_2$-η^6-pyridine]chromium **5**[6] and bis[2,4,6-$(^tBu)_3$-η^6-phosphinine]chromium **6**,[7] respectively. Not surprisingly, bulky groups in the *ortho*-position of the aromatic ring change the preference of the coordination mode from (σ, η^1)- to (π, η^6)-coordination for E = N and P.[8] In the last few years several papers were published that describe the metal coordination of substituted group 15 heteroarenes.[9] A question that has not yet been addressed concerns the possibility that within a particular group of transition elements the preferred coordination mode might change with the atomic number of M. In this context, the triad $M(tmbp)_3$ (tmbp = 4,4′,5,5′-tetramethyl-2,2′-biphosphinine; M = Cr, **7**; Mo, **8**; W, **9**) reported by Mathey et al.[10] appears to be the only series in this case. These metal chelates all feature η^1-coordination via the P atoms. In line with our predilection for unsubstituted, homoleptic parent complexes, we prepared the prototypes $Mo(\eta^1\text{-}C_5H_5P)_6$ **10** and $W(\eta^1\text{-}C_5H_5P)_6$ **11** and compared them with the lighter homologue $Cr(\eta^1\text{-}C_5H_5P)_6$ **2** described previously.[3]

† Dedicated to Professor Peter Jutzi on the occasion of his 60th birthday.

(1) Metal Complexes of Heteroarenes. 9. Part 8: see ref 4.

(2) Elschenbroich, Ch.; Nowotny, M.; Metz, B.; Graulich, J.; Massa, W.; Biehle, K.; Sauer, W. *Angew. Chem., Int. Ed. Engl.* **1991**, *30*, 547.

(3) Elschenbroich, Ch.; Nowotny, M.; Kroker, J.; Behrendt, A.; Massa, W.; Wocadlo, S. *J. Organomet. Chem.* **1993**, *459*, 157.

(4) Elschenbroich, Ch.; Nowotny, M.; Behrendt, A.; Harms, K.; Wocadlo, S.; Pebler, J. *J. Am. Chem. Soc.* **1994**, *116*, 6217.

(5) Elschenbroich, Ch.; Nowotny, M.; Behrendt, A.; Massa, W.; Wocadlo, S. *Angew. Chem., Int. Ed. Engl.* **1992**, *31*, 1343.

(6) (a) Timms, P. L. *Angew. Chem., Int. Ed. Engl.* **1975**, *87*, 295. (b) Simons, L. H.; Riley, P. E.; Davis, R. E.; Lagowski, J. J. *J. Am. Chem. Soc.* **1976**, *98*, 1044. (c) Wucherer, E. J.; Muetterties, E. L. *Organometallics* **1987**, *6*, 1691. (d) Biedermann, H. G.; Öfele, K.; Tajtelbaum, J. *Z. Naturforsch.* **1976**, *31B*, 321.

(7) Elschenbroich, Ch.; Bär, F.; Bilger, E.; Mahrwald, D.; Nowotny, M.; Metz, B. *Organometallics* **1993**, *12*, 3373.

(8) Elschenbroich, Ch.; Koch, J.; Kroker, J.; Wünsch, M.; Massa, W.; Baum, G.; Storck, G. *Chem. Ber.* **1988**, *121*, 1983.

(9) (a) Ashmore, J.; Green, J. C.; Green, M. L. H.; Smith, M. L.; Mehnert, C.; Wucherer, E. J. *J. Chem. Soc., Dalton Trans.* **1995**, 1873. (b) Mehnert, C. P.; Chernega, A. N.; Green, M. L. H. *J. Organomet. Chem.* **1996**, *513*, 247. (c) Arnold, P. L.; Cloke, F. G. N.; Khan, K.; Scott, P. *J. Organomet. Chem.* **1997**, *528*, 77. (d) Le Floch, P.; Knoch, F.; Kremer, F.; Mathey, F.; Scholz, J.; Scholz, W.; Thiele, K.-H.; Zenneck, U. *Eur. J. Inorg. Chem.* **1998**, 119. (e) Le Floch, P.; Knoch, F.; Kremer, F.; Mathey, F.; Schmidt, U.; Zenneck, U. *Organometallics* **1996**, *15*, 2713. (f) Böhm, D.; Knoch, F.; Kummer, S.; Schmidt, U.; Zenneck, U. *Angew. Chem., Int. Ed. Engl.* **1995**, *34*, 198. (g) Binger, P.; Leininger, S.; Stannek, J. ; Gabor, B.; Mynott, R.; Bruckmann, J.; Krüger, C. *Angew. Chem., Int. Ed. Engl.* **1995**, *34*, 2227. (h) Arnold, P. L.; Cloke, F. G. N.; Hitchcock, P. B.; Nixon, J. F. *J. Am. Chem. Soc.* **1996**, *118*, 7630. (i) Arnold, P. L.; Cloke, F. G. N.; Hitchcoock, P. B. *J. Chem. Soc., Chem. Commun.* **1997**, 481. (j) Breit, B. *J. Chem. Soc., Chem. Commun.* **1996**, 2071. (k) Breit, B.; Winde, R.; Harms, K. *J. Chem. Soc., Dalton Trans.* **1997**, 2681 (l) Le Floch, P.; Ricard, L.; Mathey, F.; Jutand, A.; Amatore, Ch. *Inorg. Chem.* **1995**, *34*, 11.

(10) (a) Mathey, F.; Le Floch, P. *Chem. Ber.* **1996**, *129*, 263. (b) Le Floch, P.; Mathey, F. *Coord. Chem. Rev.*, in press and references therein.

S0276-7333(98)00487-7 CCC: $15.00
Publication on Web 09/09/1998

Chart 1

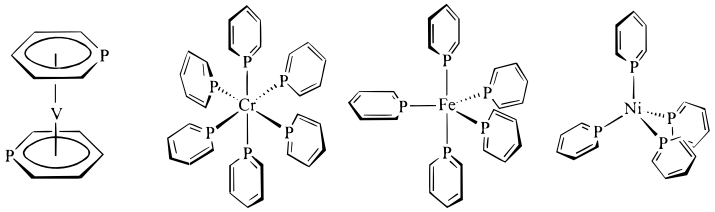

1 **2** **3** **4**

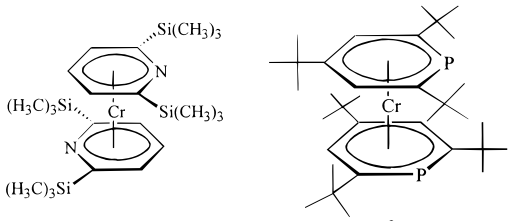

5 **6**

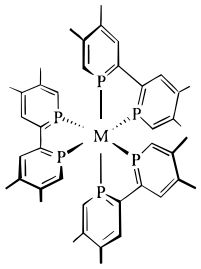

M = Cr **7**, Mo **8**, W **9**

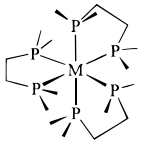

M = Cr **13**, Mo **14**, W **15**

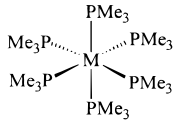

M = Mo **16**, W **17**

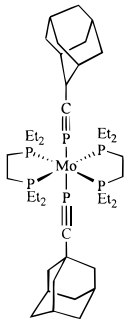

19

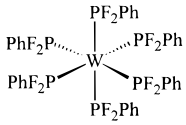

18

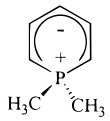

20

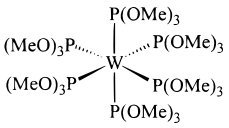

21

Results and Discussion

Hexakis(η^1-phosphinine)molybdenum **10** and hexakis(η^1-phosphinine)tungsten **11** are accessible via reduction of the respective metal halide with magnesium or zinc in the presence of phosphinine **12** following the method given for **7**−**9** (Scheme 1).[10] The new phosphinine complexes **10** and **11** are moderately air stable and resist thermal decomposition up to 300 °C. The ease of formation and the latter properties suggest that operation of the chelate effect, as in **7**−**9**, is not required, and it is the inherent nature of the transition metal−phosphinine bond that stabilizes the η^1-complexes. Note that this contrasts with pyridine as a ligand in that $(bipyridine)_3Cr$ is known whereas $(pyridine)_6Cr$ is not. It is worth mentioning that the synthesis presented in Scheme 1 failed for arsenine C_5H_5As replacing phosphinine, neither η^1- nor η^6-arsenine complex formation being evident.

According to the results of single-crystal X-ray analyses (Figures 1 and 2, Tables 1 and 7), the complexes **10** and **11** are isostructural and bear strong resemblance to **2**.[3] Both **10** and **11** display octahedral coordination of the central metal by six phosphinine ligands. In analogy to the chromium complex **2** opposite phosphinine moities are not coplanar. The torsional angles between trans disposed ligand pairs cover the range from 18.1(3)° to 85.9(3)°, which exceeds that found for **2**. Therefore, the conceivable T_h-symmetry is lowered to C_i, and the unit cell in all three cases (Cr, Mo, W) consists of four $M(\eta^1\text{-}C_5H_5P)_6$ molecules with two crystallographically independent complex units. The bond lengths M−P (M = Cr, Mo, W) follow the expected order Cr−P (2.26 Å, **2**[3]) < Mo−P (2.38 Å, **10**) ≈ W−P (2.37 Å, **11**). The same gradation is observed for $M(dmpe)_3$, M = Cr (2.31 Å, **13**[11]), M = Mo (2.42 Å, **14**), and M = W (2.41 Å, **15**[12]), which, to our knowledge, is the only

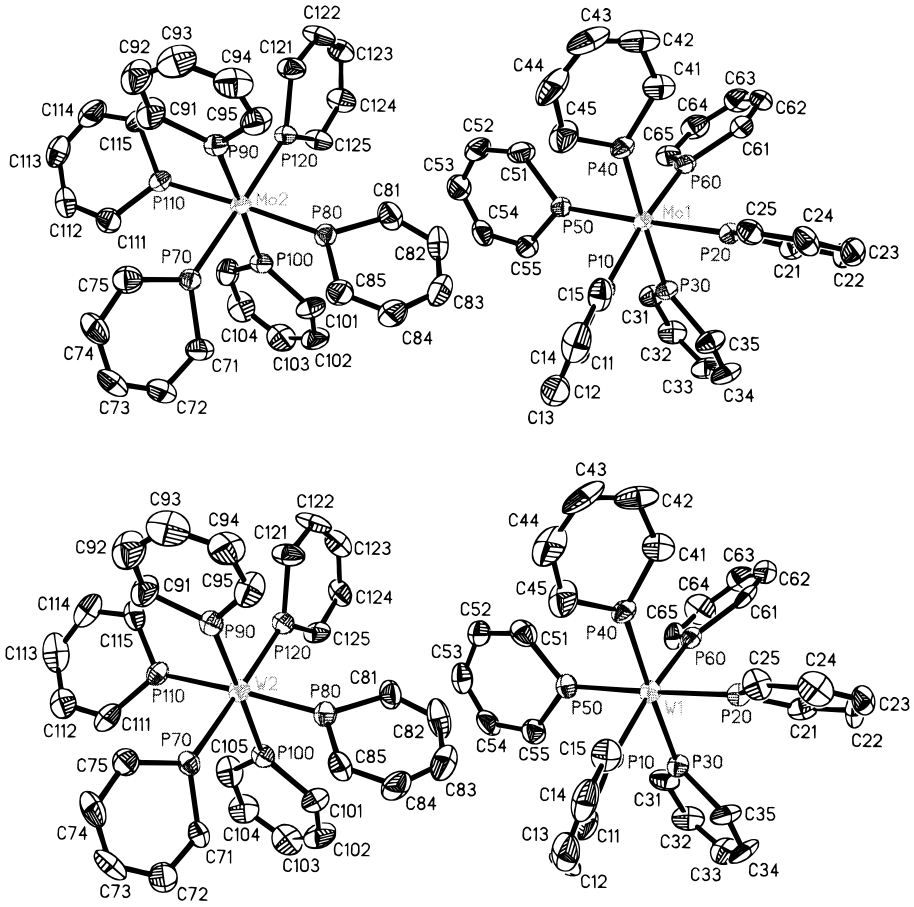

Figure 1. Molecular geometry and atom-numbering scheme for $Mo(C_5H_5P)_6$ **10** and $W(C_5H_5P)_6$ **11**.

Scheme 1

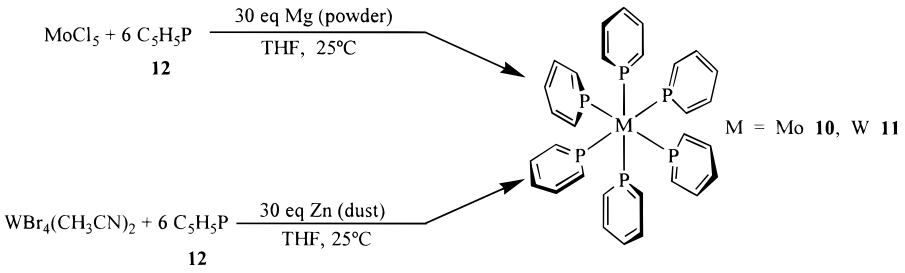

example for crystallographically characterized phosphane complexes of the whole triad Cr, Mo, and W. Compared to the M−P bond lengths in $Mo(PMe_3)_6$ **16** (2.46 Å[13]) and $W(PMe_3)_6$ **17** (2.45 Å[14]), the observed values for **10** and **11** are rather short. The W−P bond distance in **11** is nearly identical to that found in $W(PPhF_2)_6$ **18** (2.37 Å[15]), which contains the strong π-acceptor ligand $PPhF_2$, suggesting that strong M → P π-back-donation prevails in the case of the homoleptic η^1-phosphinine complexes.[3] It has to be kept in mind, however, that the hybridization of phosphorus in **12** is sp^2 versus sp^3 as in dmpe, PMe_3, or $PPhF_2$. Hence, the M−P bond length in phosphinine complexes should generally be shorter than those encountered in phosphane complexes. This effect, as an example, also accounts for the differing bond lengths in **19** (2.30 Å Mo−P(sp); 2.43 Å Mo−P (sp^3)).[16]

The ligand dimensions in **10** and **11** are affected by the η^1-coordination only marginally: while the C−P−C bond angles remain virtually unchanged, the P−C and C−C bonds are shortened only slightly. Constancy of the C−P−C bond angle had also been observed upon homoleptic η^1-coordination of phosphinine to chromium,[3] iron,[4] and nickel,[5] whereas in the heteroleptic complexes $(\eta^1\text{-}C_5H_5P)Mo(CO)_5$[17a] and $(2,6\text{-}Me_2\text{-}4\text{-}Ph\text{-}C_5H_2P)_2PtCl_2$

(11) dmpe = 1,2-bis(dimethylphosphino)ethane: Chatt, J.; Watson, H. R. *J. Chem. Soc.* **1962**, 2545.

(12) Cloke, F. G. N.; Fyne, P. J.; Gibson, V. C.; Green, M. L. H.; Ledoux, M. J.; Perutz, R. N.; Dix, A.; Gourdon A.; Prout K. *J. Organomet. Chem.* **1984**, *277*, 61.

(13) (a) Brookhart, M.; Cloke, F. G. N.; Cox, K. P.; Green, J. C.; Green, M. L. H.; Bashkin, J.; Hare, P. M.; Derome, A. E.; Grebnik, P. D. *J. Chem. Soc., Dalton Trans.* **1985**, 423. (b) Cloke, F. G. N.; Cox, K. P.; Green, M. L. H.; Bashkin, J.; Prout, K. *J. Chem. Soc., Chem. Commun.* **1982**, 393.

(14) (a) Rabinovich, D.; Zelman, R.; Parkin G. *J. Am. Chem. Soc.* **1992**, *114*, 4611. (b) Rabinovich, D.; Parkin, G. *J. Am. Chem. Soc.* **1990**, *112*, 5381.

(15) Crump, W.; Kruck, Th.; Siegers, B.; Tebbe, K. F. *Acta Crystallogr., Sect. C* **1994**, *50*, 1074.

(16) Hitchcock, P. B.; Maah, M. J.; Nixon, J. F.; Zora, J. A.; Leigh, G. J.; Bakar, M. A. *Angew. Chem., Int. Ed. Engl.* **1987**, *26*, 474.

Table 1. Selected Bond Length (pm) and Angles (deg) for the Group 6 Hexakis(phosphinine)metal Complexes $M(C_5H_5P)_6$ 2, 10, and 11 and for the Free Ligand 12

	12[19c]	**2** (M = Cr)	**10** (M = Mo)	**11** (M = W)
M−P		226.7(8)	238.1(16)	237.8(3)
P−C1	173	171(2)	172.0(6)	171.6(12)
P−C5	173	172(2)	171.7(6)	171.3(12)
C1−C2	141	141(3)	138.2(10)	137.9(17)
C2−C3	138	136(4)	136.8(10)	138.5(15)
C3−C4	138	138(3)	137.2(11)	136.0(16)
C4−C5	141	140(3)	138.2(9)	137.9(16)
$C-C_{(mean)}$	139.5(17)	138.7(22)	137.6(10)	137.6(16)
C4−C7				
$C-C_{aliph.(mean)}$				
C−H	94(2)		94.0	94.0
$P-M-P_{(cis)}$		86.0(3)−93.4(3)	86.1−94.1(6)	86.1−93.9(11)
$P-M-P_{(trans)}$		174.3−178.2(3)	174.2−178.0(6)	174.3−178.2(11)
M−P−C1		130.2(9)	129.4(2)	129.5(4)
M−P−C5		128.9(8)	129.3(2)	129.5(4)
C1−P−C5	101	101(1)	101.2(3)	101.0(6)
P−C1−C2		125(2)	124.1(5)	124.7(10)
C1−C2−C3		121(2)	124.4(6)	122.9(12)
C2−C3−C4		125(2)	122.1(6)	122.7(12)
C3−C4−C5		121(2)	124.0(6)	124.2(12)
P−C5−C4		125(2)	124.3(5)	124.5(11)

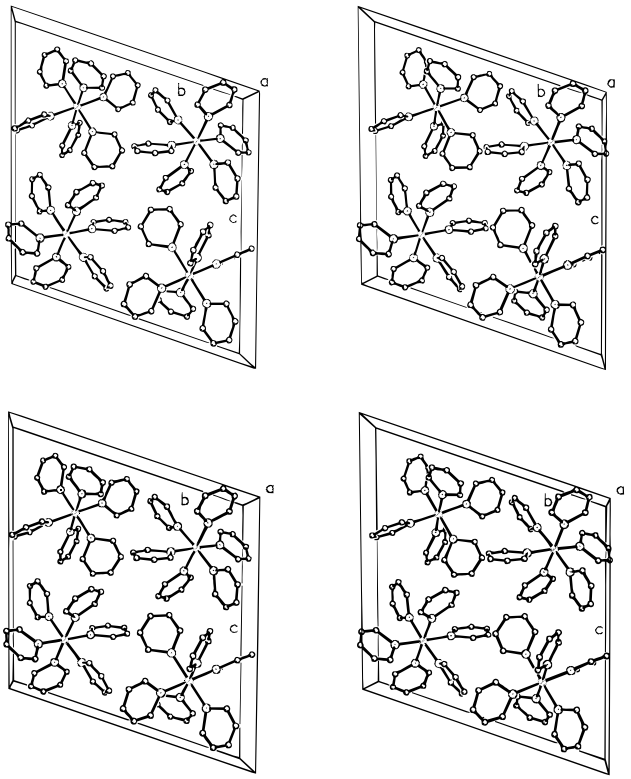

Figure 2. Stereo drawing of the unit cells of $Mo(C_5H_5P)_6$ **10** and $W(C_5H_5P)_6$ **11**.

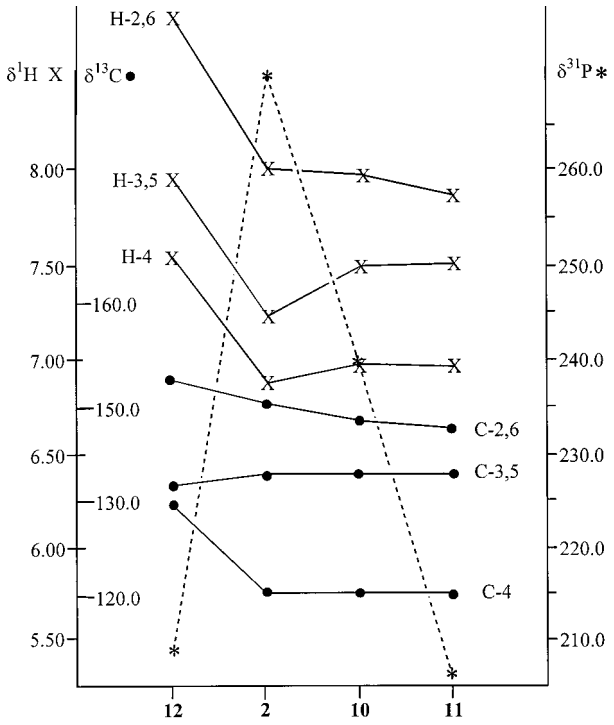

Figure 3. Trends of the ^{1}H-, ^{13}C-, and ^{31}P-NMR Data in the Triad $M(\eta^1\text{-}C_5H_5P)_6$ (M = Cr, **2**; Mo, **10**; and W, **11**).

enlargement of this angle to 103.1° and 107.7°, respectively, has been reported.[17]

The ^{1}H-, ^{13}C-, and ^{31}P-NMR data of **2**, **10**, **11**, and **12** are presented in Table 2, and the trends are depicted in Figure 3; the ^{1}H- and ^{1}H{^{31}P}-NMR spectra of **10** and **11** are shown in Figure 4. The general negative coordination shifts of the *ortho*-protons ($\Delta\delta^1$H) and the carbon atoms ($\Delta\delta^{13}$C) increase in the series Cr < Mo < W. An opposite trend is observed for the coordination shift of the phosphorus atoms ($\Delta\delta^{31}$P). It parallels the reported coordination shifts ($\Delta\delta^{31}$P) for several heteroleptic phosphane−carbonyl complexes of Cr, Mo, and W (Table 3[18]). The steadily increased shielding of the nuclei closest to the central metal (P, H-2,6, and C-2,6) in **2**, **10**, and **11** suggests that the shielding constants σ of these nuclei are governed by the shielding contribution of the neighboring group, in this case the central metal. Typically, the coordination shift of the phospho-

(17) (a) Ashe, A. J., III; Butler, W.; Colburn, J. C.; Abu-Orabi, S. *J. Organomet. Chem.* **1985**, *282*, 233. (b) Elschenbroich, Ch.; Voss, S.; Harms, K. *Z. Naturforsch. B*, submitted.

(18) (a) Mathieu, R.; Lenzi, M.; Poilblanc, R. *Inorg. Chem.* **1970**, *9*, 2030. (b) Moser, E.; Fischer, E. O.; Barthelt, W.; Gretner, W.; Knaus, L.; Louis, E. *J. Organomet. Chem.* **1969**, *19*, 382. (c) Deberitz, J.; Nöth, H. *J. Organomet. Chem.* **1973**, *49*, 453. (d) Mark, V.; Dungan, H.; Crutchfield, M. M.; van Wazer, J. R. *Topics in Phosphorus Chemistry*; Griffith, E. J., Grayson, M., Eds.; 1967; Vol. 5, p 277.

Table 2. NMR Data of Phosphinine 12, Cr(η^1-C_5H_5P)$_6$ 2,[3] Mo(η^1-C_5H_5P)$_6$ 10, W(η^1-C_5H_5P)$_6$ 11, and, for Comparison, 1,1-Dimethyl-λ^5-phosphinine 20[19] Measured in [D_8]THF at T = 298 K (Chemical Shifts δ in ppm and Coupling Constants J in Hz)

	12	2	10	11	20
δH-2,6($\Delta\delta$)[a]	8.77	8.00(−0.77)	7.98(−0.79)	7.82(−0.95)	3.98
^2J(HP)	38.5	n.r.[b]	n.r.[b]	n.r.[b]	17.1
$^3J(H_{2,6}\text{-}H_{3,5})$		11.0	10.2	10.6	
δH-3,5($\Delta\delta$)	7.87	7.41(−0.46)	7.48(−0.39)	7.49(−0.38)	6.70
^3J(HP)	8.1	n.r.[b]	n.r.[b]	n.r.[b]	34.0
$^3J(H_{3,5}\text{-}H_4)$[c]		8.0	8.0	8.0	
δH-4($\Delta\delta$)	7.55	6.85(−0.70)	6.92(−0.63)	6.87(−0.58)	4.62
^4J(HP)	3.3	n.r.[b]	n.r.[b]	n.r.[b]	7.5
δP($\Delta\delta$)	206.5	270.8(64.3)	239.5(33.0)	201.8(−4.8)	
^1J(PW)				304.0	
δC-2,6($\Delta\delta$)	155.1	151.6(−3.5)	148.7(−6.4)	146.5(−8.6)	67.5
^1J(CH)	156.3	155.0	n.r.[b]	n.r.[b]	
^1J(CP)	54.0	n.r.[b]	n.r.[b]	n.r.[b]	
δC-3,5($\Delta\delta$)	134.7	136.2(1.5)	136.1(1.4)	136.9(2.2)	139.2
^1J(CH)	154.9	152.0	n.r.[b]	n.r.[b]	
^2J(CP)	14.3	n.r.[b]	n.r.[b]	n.r.[b]	
δC-4($\Delta\delta$)	129.8	121.4(−8.4)	121.7(−8.1)	121.1(−8.7)	94.0
^1J(CH)	160.0	160.5	n.r.[b]	n.r.[b]	
^3J(CP)	22.0	n.r.[b]	n.r.[b]	n.r.[b]	

[a] Coordination shift $\Delta\delta = \delta$(complex) − δ(free ligand). [b] n.r. = not resolved. [c] Higher order spin system.

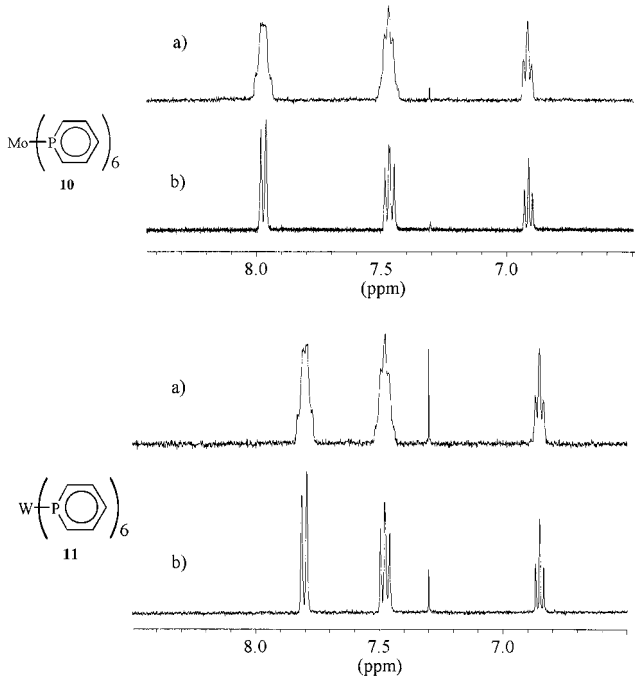

Figure 4. ^{1}H-(a) and ^{1}H{^{31}P}-NMR Spectra (b) of Mo(C_5H_5P)$_6$ **10** and W(C_5H_5P)$_6$ **11**.

Table 3. ^{31}P-NMR Data of Heteroleptic Phosphane−Carbonyl Complexes of Cr, Mo, and W (Chemical Shifts and Coordination Shifts in ppm)[18]

	$P(OCH_3)_3$	PH_3	$C_{23}H_{17}P$[a]
P	141	−239	178.2
$PCr(CO)_5$	179.6(38.6)	−129.6(109.4)	197.8(19.8)
$PMo(CO)_5$	162.0(21.0)	−165.5(73.5)	180.3(2.1)
$PW(CO)_5$	137.3(−3.7)	−187.7(51.3)	156.3(−21.9)
$P_2Cr(CO)_4$[b]	180.2(39.2)	−121.5(117.5)	216.6(38.4)
$P_2Mo(CO)_4$[b]	164.0(23.0)	−159(80)	190.5(12.3)
$P_2W(CO)_4$[b]	141.1(0.1)	−180(59)	170.5(−7.7)

[a] $C_{23}H_{17}P$ = 2,4,6-triphenylphosphinine. [b] Cis coordination of the P-ligands.

rus atom, which is directly bonded to the central metal, changes from 64.3 ppm in **2** to −4.8 ppm in **11**. Contrarily, the coordination shifts for the *meta*-(H-3,5) and *para*-(H-4) ring protons as well as the *meta*-(C-3,5) and *para*-(C-4) carbon atoms, which are more remote from the central metal, are very similar to those in **2**. On the basis of the similarity of the change in the NMR data upon moving from λ^3-phosphinine to 1,1-dimethyl-λ^5-phosphinine (**20**)[19] (Table 2), we proposed the contribution of an ylid resonance structure for the η^1-coordinated λ^3-phosphinine (Scheme 2).[1,3] This interpretation of the η^1-coordination-induced changes of the shielding properties reflects the double-bond character of the metal-to-phosphorus bond, with attendant short bond length; it applies to **2**, **3**, and **4** as well as to **10** and **11** and therefore is independent of the radius of the central metal atom. The coupling constant $^1J(^{183}W,^{31}P)$ = 304.0 Hz in **11** is in the typical range for tungsten phosphane complexes (100−800 Hz[20]). Yet, it falls short of the respective value $^1J(^{183}W,^{31}P)$ = 449 Hz for W[P(OMe)$_3$]$_6$ (**21**),[21] where the phosphane ligand bears electronegative substituents.

Scheme 2

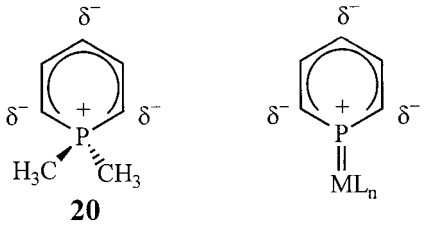

20

All three complexes **2**, **10**, and **11** give intensely colored dark red solutions in benzene or THF; they furnish very similar electronic spectra (Figure 5 and Table 4). A metal(d^6) ion in a strong octahedral field gives rise to two spin-allowed d−d transitions: $^1A_{1g} \rightarrow$

(19) (a) Ashe, A. J., III; Smith, T. W. *J. Am. Chem. Soc.* **1976**, *98*, 7861. (b) Ashe, A. J., III; Jones, G. J.; Miller, F. A. *J. Mol. Struct.* **1982**, *78*,169. (c) Ashe, A. J. *Acc. Chem. Res.* **1978**, *11*, 153.
(20) (a) Hesse, M.; Meier, H.; Zeeh, B. *Spektroskopische Methoden in der Organischen Chemie*, 4. Aufl.: Georg Thieme Verlag: Stuttgart, 1991. (b) Berger, S.; Braun, S.; Kalinowski, H. O. *NMR-Spektroskopie von Nichtmetallen*, Bd. 3; Georg Thieme Verlag: Stuttgart, 1993.
(21) Muetterties, E. L.; Choi, H. W. *J. Am. Chem. Soc.* **1982**, *104*, 153.

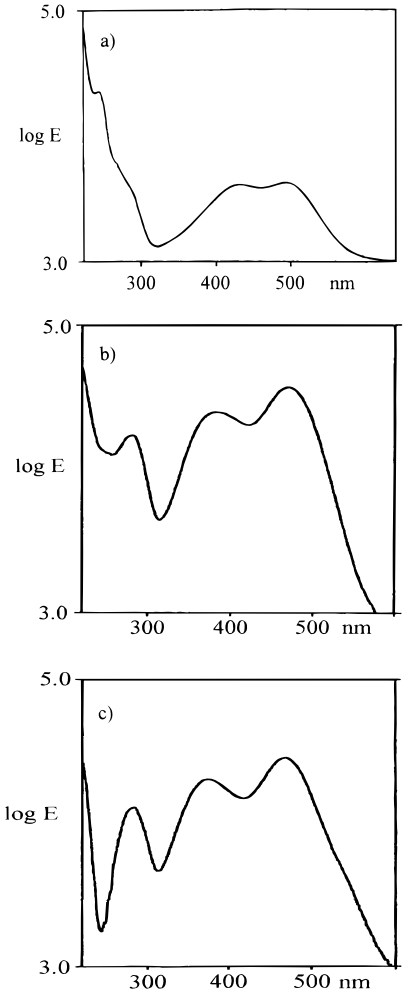

Figure 5. Electronic spectra of **2** (a), **10** (b), and **11** (c) in THF.

Table 4. UV−Vis Data of 12, 2,[3] 10, and 11 in THF

complex	λ_{max} [nm][a]	ϵ [L mol^{-1} cm^{-1}]	transition
C_5H_5P[b] **12**	213	19 000	$\pi \rightarrow \pi^*$
	246	8500	$\pi \rightarrow \pi^*$
	268sh	250	n $\rightarrow \pi^*$
(η^1-$C_5H_5P)_6$Cr **2**	244 (246)	40 000	$\pi \rightarrow \pi^*$
	284sh (288)	20 000	$\pi \rightarrow \pi^*$
	430 (443)	18 400	$t_{2g} \rightarrow \pi^*$ (MLCT)
	492 (∼510sh)	18 800	$t_{2g} \rightarrow \pi^*$ (MLCT)
(η^1-$C_5H_5P)_6$Mo **10**	280 (270)	23 600	$\pi \rightarrow \pi^*$
	382 (369)	33 300	$t_{2g} \rightarrow \pi^*$ (MLCT)
	481 (465)	47 600	$t_{2g} \rightarrow \pi^*$ (MLCT)
(η^1-$C_5H_5P)_6$W **11**	281 (270)	19 000	$\pi \rightarrow \pi^*$
	373 (373)	27 700	$t_{2g} \rightarrow \pi^*$ (MLCT)
	468 (467)	37 400	$t_{2g} \rightarrow \pi^*$ (MLCT)

[a] Values in parentheses are for methylcyclohexane as solvent. [b] Solvent = C_6H_{12}.

$^1T_{1g}$ and $^1A_{1g} \rightarrow {}^1T_{2g}$.[22] However, as in the case of **2**, MLCT absorptions due to low lying π^*-orbitals of the phosphinine ligands[23] also have to be considered. Accordingly, in the visible region, **10** and **11** show two strong absorptions with large extinction coefficients but small solvatochromic effects. These absorptions exhibit hypsochromic shifts along the sequence Cr < Mo < W,

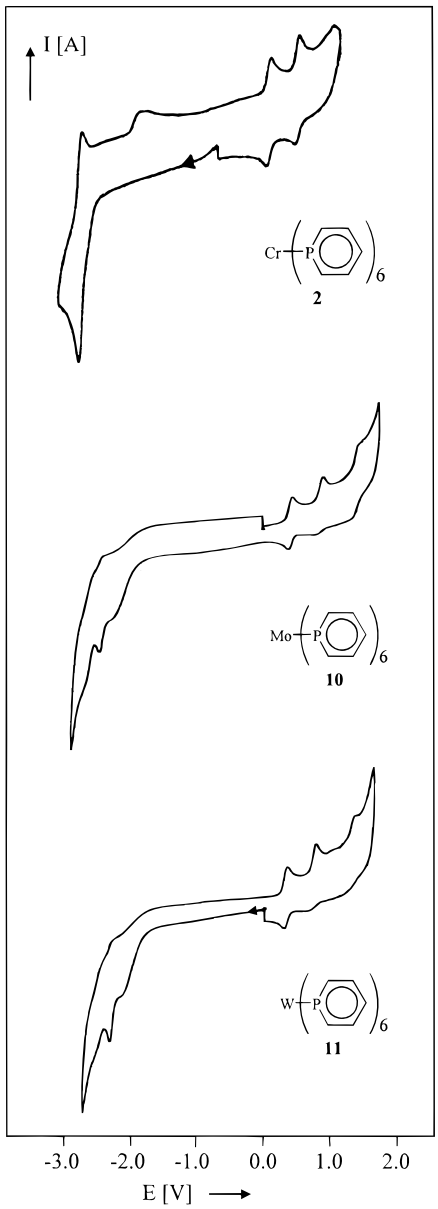

Figure 6. Cyclic voltammograms for **2**, **10**, and **11** in DME/Bu_4NClO_4 at −40 °C, 100 mV/s.

which may be rationalized in terms of the increase of the first ionization energies of the free metals, IE (M→M$^+$, kJ/mol) = 653 (Cr), 685 (Mo), 770 (W).[24] The absorption at 280 nm is virtually unaffected by the change of the central metal, and it is assigned to an intraligand ($\pi \rightarrow \pi^*$) transition.[3]

The redox properties of the homoleptic phosphinine complexes **2**, **10**, and **11** were studied by cyclic voltammetry (CV); electrochemical traces are depicted in Figure 6. The reductions of **10** and **11** are dominated by large cathodic waves, which, based on a comparison with the CV of authentic material, are characteristic for the free ligand **12** (Table 5). In their reduction behavior **10** and **11** strongly resemble **2**. However, in contrast to **2**, irreversible reduction of **10** and **11** can be observed as an anodic shoulder at the reduction wave for **12**. The irreversible nature of this process reflects the instability

(22) Verkade, J. G. *Coord. Chem. Rev.* **1972**, *9*, 1.
(23) Waluk, J.; Klein, H.-P.; Ashe, A. J., III; Michl, J. *Organometallics* **1989**, *8*, 2804.
(24) Emsley, J. *The Elements*, 2nd ed.; Clarendon Press: Oxford, 1991.

Table 5. Cyclovoltammetric Data for the Complexes 2, 10, and 11

	2	10	11
$E_{pc}(0/-)^{a,e}$	−2.28	−2.28	−2.28
$E_{pa}(0/-)^{b,e}$	−2.22	−2.22	−2.22
$\Delta E_p{}^{c,e}$	66	66	66
$r^{d,e}$	0.57	0.57	0.57
n	1	1	1
E_{pa}(ECE)	−1.42		
$E_{pc}(0/-)$		−1.91[f]	−1.946[f]
$E_{1/2}(+/0)$	0.14[h]	0.360[g]	0.290[g]
$E_{pa}(+/0)$	0.17	0.388	0.320
$E_{pc}(+/0)$	0.11	0.332	0.260
ΔE_p	60	56	60
r	1.1	1.0	1.0
n	1	1	1
$E_{pa}(2+/+)$	0.52[i]	0.776[f]	0.712[f]
$E_{pc}(2+/+)$	0.46	0.724	0.662
ΔE_p	69	52	90
r	1.4	6.0	4.5
$E_{pa}(3+/2+)$	0.93[f]		0.952[f]

[a] Cathodic potential [V]. [b] Anodic potential [V]. [c] Peak separation $\Delta E_p = E_{pa} - E_{pc}$ [mV]. [d] $r = I_{pa}/I_{pc}$. [e] Values are identical to free **12**. [f] Irreversible process. [g] Quasireversible process. [h] Reversible process. [i] Irreversible at slow scan rates (v < 100 mV/s).

Table 6. Redox Potentials $E_{1/2}(0/+)$ (V) of Homoleptic Carbonyl,[26] Phosphinine, and 2,2′-Bipyridyl Complexes[27] of Group 6 Metals

	CO	C_5H_5P	bpy
Cr	1.43[a,d]	0.14[a,e]	−1.13[a,f]
Mo	1.53[c,d]	0.36[b,e]	−1.33[a,f]
W	1.53[c,d]	0.29[b,e]	

[a] Reversible process. [b] Quasireversible process. [c] Irreversible process (E_{pc} is given). [d] In CH_2Cl_2/TBAP vs SCE. [e] In DME/TBAP vs SCE. [f] In CH_3CN/TBAP vs SCE.

of the 19-VE species generated, a feature that is typical for all known homoleptic η^1-phosphinine complexes.[3−5] Obviously, **12** is not able to support an additional negative charge in these homoleptic η^1-complexes. It should be mentioned, however, that the stability of homoleptic phosphinine transition metal radical anions is somewhat increased if the phosphinine unit is part of a chelating ligand.[10] Whereas the process $\mathbf{2}^{(+/0)}$ is reversible, the first oxidation of **10** and **11** must be termed quasireversible. Furthermore, the processes $\mathbf{10}^{(2+/+)}$ and $\mathbf{11}^{(2+/+)}$ are completely irreversible, while the process $\mathbf{2}^{(2+/+)}$ was irreversible only for low scan rates (v < 100 mV/s).[3] The loss of electrons from the t_{2g} set, which is mainly metal in character,[25] leads to a contraction of the metal orbitals and, hence, to a decrease in M → P back-bonding. Furthermore, Mo and W can increase their coordination number from six to seven, opening up an avenue for nucleophilic ligand displacement, which would account for the irreversible processes $\mathbf{10}^{(2+/+)}$ and $\mathbf{11}^{(2+/+)}$.[26] All redox processes display anodic shifts upon substitution of Cr by Mo or W. The same gradation is observed for the couples $M^{(+/0)}$ of the homoleptic carbonyl and bipyridyl complexes of the group 6 elements (Table 6).[26,27] A comparison of the redox potentials for the couples $MoL_6{}^{(+/0)}$ underlines the disparate ability of these ligands to stabilize the Mo(0) oxidation state. Obviously, phosphinine is a stronger σ-donor and/or a weaker π-acceptor than CO, while the opposite applies in a comparison of phosphinine with bipy. A similar conclusion had been reached for 4,4′,5,5′-tetramethyl-2,2′-biphosphinine in $Ni(tmbp)_2$.[10]

Table 7. Crystallographic Data and Refinement Parameters for $Mo(C_5H_5P)_6$ 10 and $W(C_5H_5P)_6$ 11

	10	11
formula	$C_{30}H_{30}MoP_6$	$C_{30}H_{30}P_6W$
fw	672.3	760.21
cryst size, mm	0.6 × 0.3 × 0.3	0.5 × 0.3 × 0.1
cryst syst	triclinic	triclinic
space gp	$P\bar{1}$	$P\bar{1}$
a, Å	9.171(1)	9.168(2)
b, Å	18.282(2)	18.318(2)
c, Å	19.142(2)	19.158(2)
α, deg	108.40(10)	108.367(9)
β, deg	95.72(10)	95.753(10)
γ, deg	90.54(10)	90.602(10)
V, Å^3	3027.3(6)	3035.1(7)
Z	4	4
D_{calcd}, Mg/m^3	1.475	1.664
$F(000)$	1368	1496
μ, cm^{-1}	7.69	41.41
temp, K	223	223
no. of data collectd	7365	8430
no. of unique data	7175	7385
no. of unique data with $I \geq 2.0\sigma(I)$	4921	5071
R index (all data)	0.0874	0.1051
R index conventional [$I > 2\sigma(I)$]	0.0422	0.0452

Experimental Section

All manipulations were carried out under an atmosphere of dry prepurified nitrogen. The solvents were purified by conventional methods. They were freshly distilled and thoroughly degassed prior to use. Instrumental analysis: ^{1}H-NMR, Bruker AMX-500 (500.13 MHz), ^{13}C- and ^{31}P-NMR, DRX-400 (100.61 and 125.77 MHz, respectively). NMR measurements were performed on solutions in sealed tubes. MS: Varian MAT, CH7A (EI, 70 eV). Cyclic voltammetry: Amel 552 potentiostat, 566 function generator, and 563 multipurpose unit, Nicolet 2090-1 digital storage oscilloscope, Kipp and Zonen BD 90X/Y recorder, glassy carbon working electrode, Pt wire counter electrode, saturated aqueous calomel reference electrode coupled to the sample solution via a nonaqueous salt bridge. Cyclic voltammetry was performed under argon protection. IR spectra were recorded as KBr pellets (4000−500 cm^{-1}) and nujol mulls (500−100 cm^{-1}) on an Interferometer IFS 88 (Bruker). Electronic spectra were recorded on a Hitachi U-3410 spectrometer for 10^{-5} M solutions. Phosphinine was prepared by the literature procedure.[28]

Hexakis(η^1-phosphinine)molybdenum (10). A solution of molybdenum pentachloride (190 mg, 0.7 mmol) in 50 mL of THF was added dropwise at room temperature to a vigorously stirred suspension of phosphinine (420 mg, 4.4 mmol) and magnesium powder (500 mg, 20 mmol) in 50 mL of THF. The light green suspension was stirred at room temperature for 24 h while the color changed to dark red. The volatiles were removed under vacuum, and the resultant red residue was extracted with 100 mL of benzene. Filtration through alumina/5% H_2O yielded a moderately air sensitive solution, which was concentrated under vacuum and layered with 30 mL of *n*-hexane. Crystallization at room temperature after two weeks yielded 150 mg of **10** (0.22 mmol, 32% based on $MoCl_5$) as green shiny, moderately air sensitive needles. IR: 2998

(25) Beach, N. A.; Gray, H. B. *J. Am. Chem. Soc.* **1968**, *90*, 5713.
(26) (a) Pickett, C. J.; Pletcher, D. *J. Chem. Soc., Dalton Trans.* **1975**, 879. (b) Bohling, D. A.; Evans, J. F.; Mann, K. R. *Inorg. Chem.* **1982**, *21*, 3546.
(27) (a) Hughues, M. C.; Macero, D. J. *Inorg. Chem.* **1976**, *15*, 2040. (b) DuBois, D. W.; Iwamoto, R. W.; Kleinberg, J. *Inorg. Chem.* **1970**, *9*, 968.
(28) Ashe, A. J., III *J. Am. Chem. Soc.* **1971**, *93*, 3293.

vw, 2956 w, 1601 w, 1542 s, 1501 s, 1382 vs, 1276 m, 1174 m, 1085 m, 907 w, 855 w, 804 vw, 768 vs, 688 vs, 583 s, 473 vs, 390 w, 238 s, 117 vw. EI-MS (70 eV); *m/z* (%): 96 (100) [L^+], 70 (29) [$L^+ - C_2H_2$]; L = C_5H_5P. $C_{30}H_{30}MoP_6$ (672.351): calcd C 53.59, H 4.50; found C 53.62, H 4.42.

X-ray Crystallographic Study of 10. Data were collected on a Enraf Nonius CAD4 diffractometer with Mo Kα radiation (λ = 0.710 73 Å) and a graphite monochromator. The crystal structure was solved by direct methods and refined by the full-matrix least-squares methods (Table 7).

Hexakis(η^1-phosphinine)tungsten (11). A suspension of 123 mg (0.2 mmol) of $WBr_4(CH_3CN)_2$ in 50 mL of THF was stirred for 0.5 h. The solvent was removed under vacuum, and the residue was suspended in 50 mL of THF. The resulting suspension was added dropwise at room temperature to a suspension of 121 mg (1.3 mmol) of phosphinine and 412 mg (6.3 mmol) of zinc powder in 50 mL of THF. The dark brown suspension was stirred for 24 h at room temperature while the color changed to dark red. The volatiles were removed under vacuum, and the resultant red residue was extracted with 100 mL of benzene. Filtration through alumina/5% H_2O yielded a moderately air sensitive solution. The solution was concentrated under vacuum and covered with 50 mL of *n*-hexane. Crystallization at room temperature after three weeks yielded 50 mg (66 μmol, 32% based on $WBr_4(CH_3CN)_2$) of **11** as green, moderately air sensitive cubes displaying a metallic luster. IR: 3026 w, 3000 w, 2963 w, 1722 w, 1597 w, 1543 s, 1503 s, 1477 w, 1384 s, 1276 m, 1263 m, 1173 m, 1087 m, 1025 m, 907 m, 859 w, 802 m, 766 s, 689 vs, 585 s, 472 vs, 393 w, 273 w, 118 vw. MS (70 eV); *m/z* (%): 96 (100) [L^+], 70 (25) [$L^+ - C_2H_2$]; L = C_5H_5P. $C_{30}H_{30}P_6W$ (760.27): calcd C 47.40, H 3.98; found C 47.51, H 4.13.

X-ray Crystallographic Study of 11. Data were collected on a Siemens P4 diffractometer with Mo Kα radiation (λ = 0.710 73 Å) and a graphite monochromator. The crystal structure was solved by direct methods and refined by the full-matrix refinement at F^2 (Table 7).

Acknowledgment. We are grateful to the Deutsche Forschungsgemeinschaft, the Volkswagen Stiftung and the Fonds der Chemischen Industrie for support of this work.

OM9804879